Journal of Ceramic Processing Research. Vol. 11, No. 4, pp. 503~507 (2010)

J O U R N A L O F
Ceramic Processing Research

Rapid consolidation of nanostructured $MoSi_2$ by pulsed current activated sintering

Seung-Myoung Chae[a], In-Yong Ko[a], Kee-Seok Nam[b] and In-Jin Shon[a,c,*]

[a]*Division of Advanced Materials Engineering, the Research Center of Advanced Materials Development, Chonbuk National University, 664-14 Deokjin-dong 1-ga, Deokjin-gu, Jeonju, Jeonbuk 561-756, Republic of Korea*

[b]*Korea Institute of Materials Science 531 Changwondaero, Changwon, Gyeongnam, 641-831, Korea*

[c]*Department of Hydrogen and Fuel Cells Engineering, Specialized Graduate School, Chonbuk National University, 664-14 Deokjin-dong 1-ga, Deokjin-gu, Jeonju, Jeonbuk 561-756, Republic of Korea*

A nanopowder of $MoSi_2$ was synthesized from Mo+2Si during high energy ball milling for 20 h. Dense nanostructured $MoSi_2$ was sintered from the mechanically activated powder within 2 minutes using pulsed current activated sintering. The average grain size of the $MoSi_2$ sample was approximately 63 nm. The hardness and fracture toughness of the sample also were investigated.

Key words: Nanostructured material, Powder metallurgy, Sintering, Mechanical properties, $MoSi_2$.

Introduction

Silicides have often been investigated as potential materials for high temperature structural applications and for application in the electronics industry. Among these, $MoSi_2$ has received considerably more attention with regard to high-temperature applications. Its properties provide a desirable combination of a high melting temperature (2020 ºC), high modulus (440 GPa), good oxidation resistance in air, a relatively low density (6.24 g/cm^3) [1], and the ability to undergo plastic deformation above 1200 ºC [2]. Combined with good thermal and electric conductivities, these properties have led to the utilization of $MoSi_2$ as a heating element material in high-temperature furnaces operating in air up to about 1700 ºC [3, 4]. However, as in the case of many such compounds, there is considerable concern regarding its low fracture toughness below the ductile-brittle transition temperature [5, 6]. To improve on their mechanical properties, the approach commonly utilized has been the addition of a second phase to form composites and nanostructured materials [7-12].

Nanostructured materials have been widely investigated because they display a wide functional diversity and exhibit enhanced or different properties compared with bulk materials [13]. Particularly, in the case of nanostructured ceramics, the presence of a large fraction of grain boundaries can lead to unusual or better mechanical, electrical, optical, sensing, magnetic, and biomedical properties [14-19]. In recent days, nanocrystalline powders have been developed by the thermochemical and thermomechanical process named the spray conversion process (SCP), by co-precipitation and high energy milling [20-22]. However, the grain size in sintered materials becomes much larger than that in pre-sintered powders due to the fast grain growth during a conventional sintering process. Therefore, even though the initial particle size is less than 100 nm, the grain size increases rapidly up to 500 nm or larger during conventional sintering [23]. So, controlling the grain growth during sintering is one of the keys to the commercial success of nanostructured materials. In this regard, the pulsed current activated sintering (PCAS) method which can make dense materials within 2 minutes, has been shown to be effective in achieving this goal [24, 25].

This paper reports an investigation of the consolidation of dense nanostructured $MoSi_2$ within 1 minute starting with the reacted nanopowder. The microstucture and mechanical properties of the resulting nanostructured $MoSi_2$ were evaluated.

Experimental Procedures

Powders of 99.9% molybdenum (<2 μm, Alfa Products) and 99% pure silicon (–325 mesh, Aldrich Products) were used as the starting materials. Mo and Si powder mixtures were first milled in a high-energy ball mill (Pulverisette-5 planetary mill) at 250 rpm for 20 h. Tungsten carbide balls (5 mm in diameter) were used in a sealed cylindrical stainless steel vial in an argon atmosphere. A charge ratio (ratio of mass of balls to powder) of 30 : 1 was used.

Fig. 1 shows the X-ray diffraction (XRD) patterns of the raw materials and milled powder. During milling, $MoSi_2$ was synthesized from Mo and 2Si powders, as shown in Fig. 1(c). The interaction between the Mo and 2Si during milling is thermodynamically feasible according to the following reaction as shown in Fig. 2:

*Corresponding author:
Tel : +82-63-270-2381
Fax: +82-63-270-2386
E-mail: ijshon@chonbuk.ac.kr

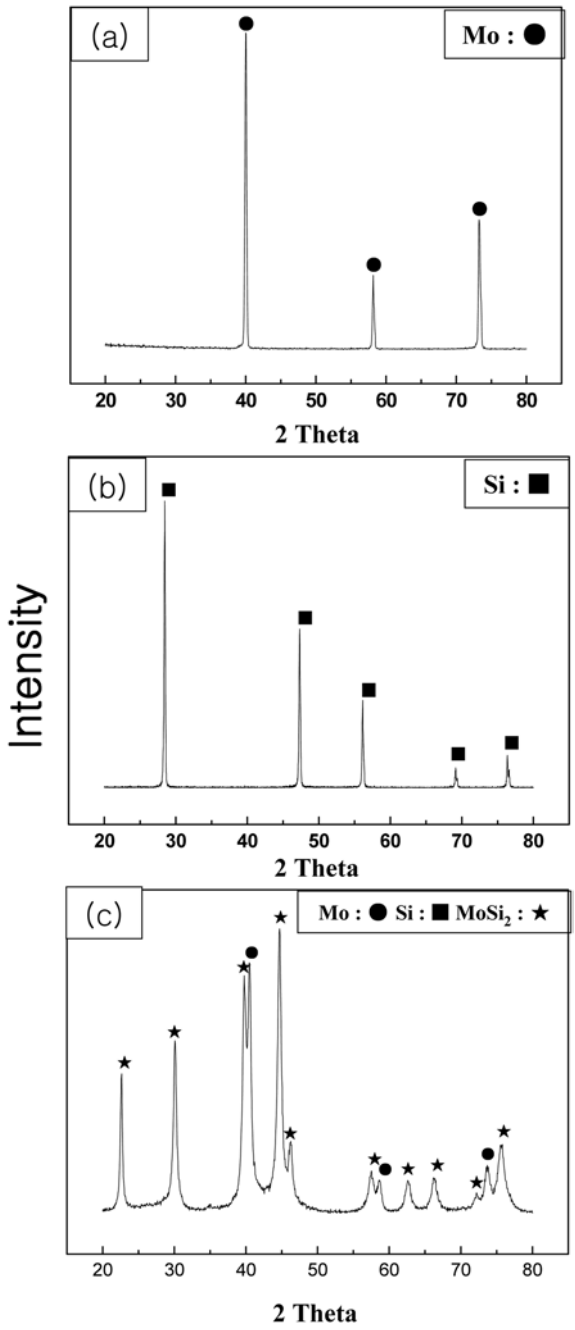

Fig. 1. XRD patterns of the raw materials : (a) Mo, (b) Si and (c) milled Mo + 2Si.

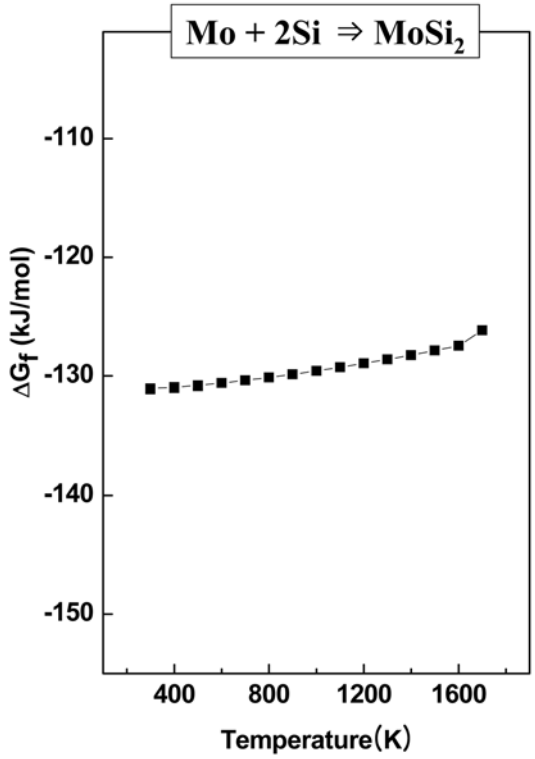

Fig. 2. Temperature dependence of the Gibbs free energy variation by interaction of molybdenum with silicon.

$$Mo + 2Si \rightarrow MoSi_2 \quad (1)$$

The grain size and internal strain were calculated using Suryanarayana and Grant Norton's formula [26] :

$$B_r(B_{crystalline} + B_{strain})\cos\theta = k\,\lambda/L + \eta\sin\theta \quad (2)$$

where B_r is the full width at half-maximum (FWHM) of a diffraction peak after an instrumental correction; $B_{crystalline}$ and B_{strain} are FWHM caused by the small grain size and internal stress, respectively; k is a constant (with a value of 0.9); λ is the wavelength of the X-ray radiation; L and η are the grain size and internal strain, respectively; and θ is the Bragg angle. The parameters, B and B_r, follow the Cauchy's form with the relationship: $B = B_r + B_s$, where B and B_s are the FWHM of the broadened Bragg peaks and the standard Bragg peaks of the samples, respectively. The mean grain size of $MoSi_2$ determined using Suryanarayana and Grant Norton's formula was approximately 31 nm.

After milling, the powder was placed in a graphite die (outside diameter = 45 mm, inside diameter = 20 mm, and height = 40 mm) and introduced into a pulsed current activated sintering system, which is shown schematically in reference [24]. The syntering was performed in four major stages. The system was evacuated to 40 mtorr (5.33 Pa) (stage 1), and a uniaxial pressure of 80 MPa was then applied (stage 2) followed by the activation of an pulsed current (on time ; 20 μs, off time ; 10 μs), which was maintained until densification was achieved, as indicated by a linear gauge measuring the shrinkage of the sample (stage 3). The temperatures were measured using a pyrometer focused on the surface of the graphite die. At the end of the process, the sample was cooled to room temperature (stage 4).

The relative density of the sintered sample was measured using the Archimedes method. Microstructural information was obtained from the product samples that had been polished and etched for 8 s at room temperature using a solution of HF (60 vol.%), HNO_3 (15 vol.%), and H_2O (25 vol.%). The composition and microstructure of the products were determined by XRD and scanning electron

microscopy (SEM) with energy dispersive X-ray analysis (EDAX). The Vickers hardness was measured by performing indentations on the sintered samples at a 5 kg load with a dwell time of 15 s.

Results and Discussion

Fig. 3 shows the changes in shrinkage displacement and temperature of the surface of the graphite die with heating time during the sintering of $MoSi_2$. As the pulsed current was applied, the specimen initially showed small (thermal) expansion, and shrinkage displacement increased gradually with temperature to approximately 800 °C, and then continuously to 1100 °C. The XRD pattern of the specimen heated to 1170 °C (Fig. 4) show only the peaks pertaining to $MoSi_2$. A structural parameter, i.e. the average grain size of the silicide phases was estimated using Suryanarayana and Grant Norton's formula [26]. Fig. 5 shows a plot of $B_r\sin\theta$ as a function of $\cos\theta$. The intercept ($k\lambda/L$) can be used to calculate the crystallite size(L). The average grain sizes of $MoSi_2$ prepared using this method were approximately 63 nm. Fig. 6 shows a FE-SEM image of the specimen heated to 1170 °C. $MoSi_2$ consisted of nanograins.

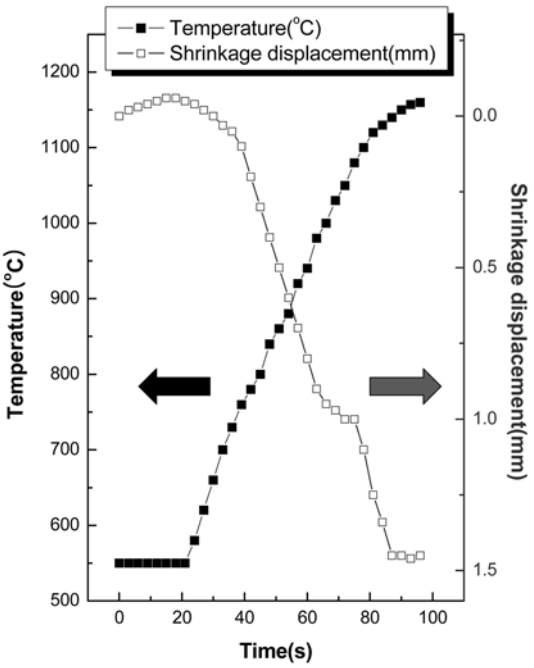

Fig. 3. Variations of temperature and shrinkage displacement with heating time during the pulsed current activated sintering of $MoSi_2$.

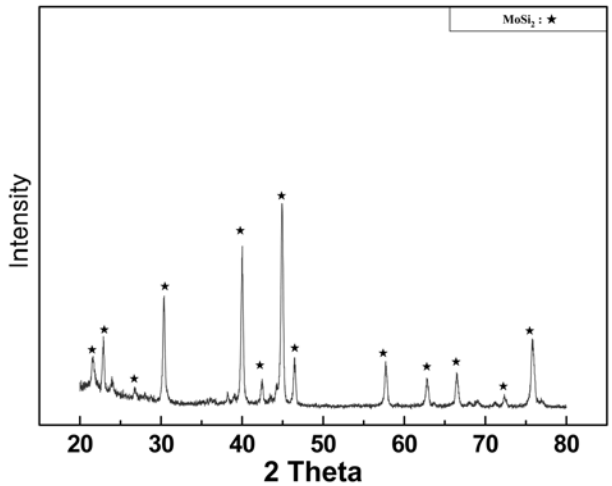

Fig. 4. XRD pattern of the $MoSi_2$ heated to 1170 °C.

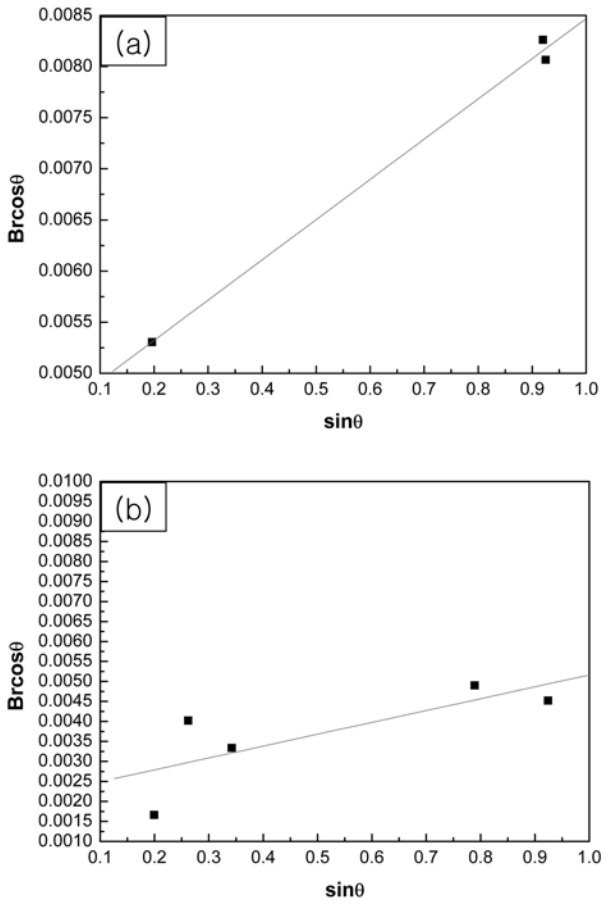

Fig. 5. Plot of $B_r\cos\theta$ versus $\sin\theta$, (a) after milling, and (b) after the consolidation of $MoSi_2$.

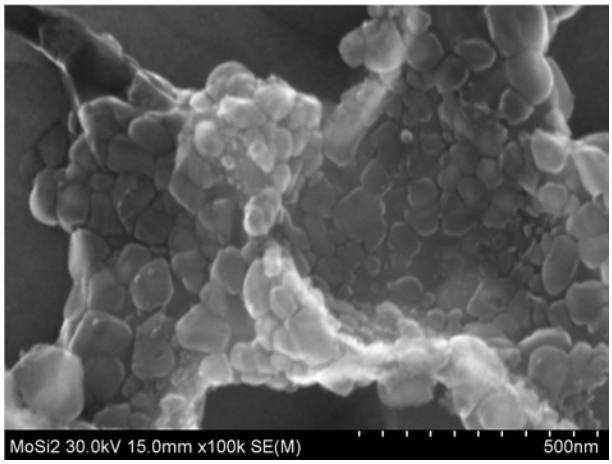

Fig. 6. FE-SEM image of the $MoSi_2$ heated to 1170 °C.

Vickers hardness measurements were made on polished sections of the $MoSi_2$ using a 5 kg_f load and 15 s dwell time. The calculated hardness value of $MoSi_2$ was 1325 kg/mm^2. This value represents an average of five measurements. Indentations with large enough loads produced median cracks around the indent. The length of these cracks permits an estimation of the fracture toughness of the materials by means of the expression [27]:

$$K_{IC} = 0.016\ (E/H)^{1/2} \cdot P/C^{3/2} \quad (3)$$

where E is Young's modulus, H is the indentation hardness, P is the indentation load, and C is the trace length of the crack measured from the center of the indentation.

A typical indentation pattern for the $MoSi_2$ is shown in Fig. 7(a). Typically, one to three additional cracks were observed to propagate from the indentation corner. The calculated fracture toughness value for the $MoSi_2$ sample is approximately 3.9 $MPa \cdot m^{1/2}$. As in the case of the hardness value, the toughness values are an average of five measurements. A higher magnification view of the indentation median crack in the $MoSi_2$ is shown in Fig. 7(b). This shows the crack deflected at several points (↑). These fracture toughness and hardness values of nanostuctured $MoSi_2$ are higher than those (fracture toughness; 2.58 $MPa \cdot m^{1/2}$ hardness; 8.7 MPa) of microstructured $MoSi_2$ [28] due to the refinement of the grain size.

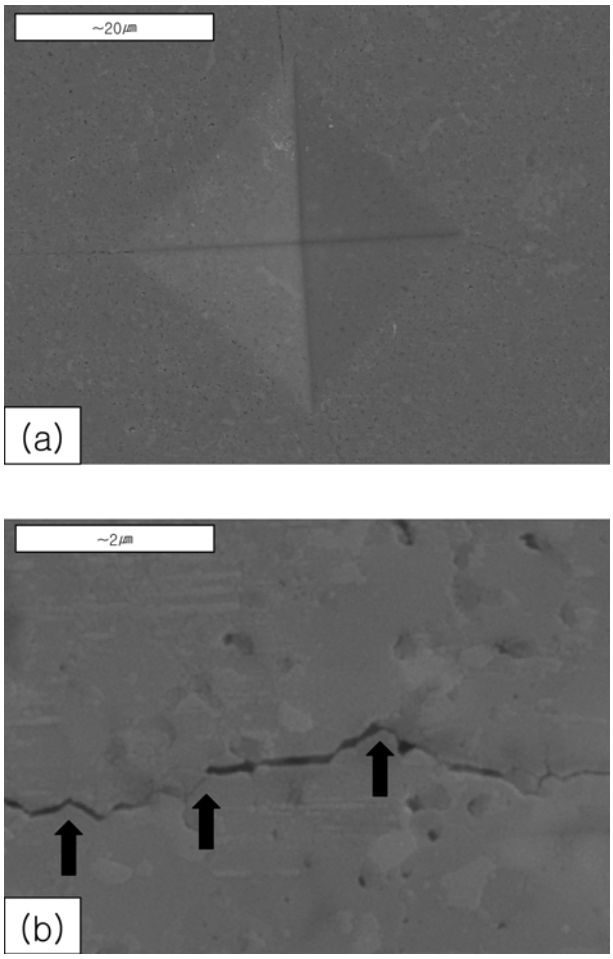

Fig. 7. (a) Vickers hardness indentation and (b) crack propagation in $MoSi_2$.

Summary

$MoSi_2$ was consolidated within 2 minutes from mechanically-activated powders using PCAS. The relative density of the $MoSi_2$ was 98% of the theoretical value at an applied pressure of 80 MPa. The average grain size of $MoSi_2$ prepared by the PCAS method was approximately 63 nm. The average hardness and fracture toughness were 1325 kg/mm^2 and 3.9 $MPa \cdot m^{1/2}$, respectively. These fracture toughness and hardness of the nanostuctured $MoSi_2$ were higher than those of microstuctured $MoSi_2$.

Acknowledgements

This work was supported by the Korea Research Foundation (KRF) grant funded by the Korean Government (MEST) (No. 2009-0065776).

References

1. A.K. Vasudevan and J.J. Petrovic, Mater. Sci. Eng. A155 (1992) 259-265.
2. R. Mitra, Y.R. Mahajan, N.E. Prasad, W.A. Chiou and C. Ganguly, Key Eng. Mater. 108-110 (1995) 11-16.
3. J. Milne, Instant Heat, Kinetic Metals Inc., Derby, Connecticut, 1985.
4. Y.S. Touloukian, R.W. Powell, C.Y. Ho and P.G. Klemens, Thermal Conductivity, IFI/Plenum, New York, 1970.
5. G. Sauthoff, Intermetallics, VCH Publishers, New York, 1995.
6. Y. Ohya, M.J. Hoffmann and G. Petzow, J. Mater. Sci. Lett. 12 (1993) 149-155.
7. B.W. Lin and T. Iseki, Br. Ceram. Trans. J. 91 (1992) 1-6.
8. Y. Ohya, M.J. Hoffmann and G. Petzow, J. Am. Ceram. Soc. 75 (1992) 2479-2456.
9. S.K. Bhaumik, C. Divakar, A.K. Singh and G.S. Upadhyaya, J. Mater. Sci. Eng. A 279 (2000) 275-281.
10. D.K. Jang and R. Abbaschian, Kor. J. Mater. Res. 9 (1999) 92-96.
11. H. Zhang, P. Chen, M. Wang and X. Liu, Rare Metals 21 (2002) 304-309.
12. D.Y. Oh, H.C. Kim, J.K. Yoon and I.J. Shon, J. Alloys & Compounds 395 (2005) 174-179.
13. H. Gleiter, Nanostruct. Mater. 6 (1995) 3-9.
14. J. Karch, R. Birringer and H. Gleiter. Nature 330 (1987) 556-561.
15. A.M. George, J. Iniguez and L. Bellaiche, Nature 413 (2001) 54-59.
16. C.W. Nahm, C.J. Kim, Y.J. Park, B.J. Lee and B.W. Park, Electron. Mater. Lett. 4 (2008) 5-11.
17. C. Xu, J. Tamaki, N. Miura and N. Yamazoe, Sens. Actuators B3, (1991) 147-155.
18. D.G. Lamas, A. Caneiro, D. Niebieskikwiat, R.D. Sanchez. D. Garcia, B. Alascio and J. Magn. Mater. 241 (2002) 207-213.
19. E.S. Ahn, N.J. Gleason, A. Nakahira and J.Y. Ying, Nano Lett. 1 (2001) 149-155.
20. Z. Fang and J.W. Eason, Int. J. of Refractory Met. & Hard

Mater. 13 (1995) 297-303.
21. A.I.Y. Tok, I.H. Luo and F.Y.C. Boey, Matrials Science and Engineering A 383 (2004) 234-239.
22. I.J. Shon, D.K. Kim, I.Y. Ko, J.K. Yoon and K.T. Hong, Mater. Sci. For. 534 (2007) 525-259.
23. M. Sommer, W.D. Schubert, E. Zobetz and P. Warbichler, Int. J. of Refractory Met. & Hard Mater. 20 (2002) 41-46.
24. I.J. Shon, D.K. Kim, K.T. Lee and K.S. Nam, Metals and Materials International. 14 (2008) 593-598.
25. S.K Bae, I.J. shon, J.M doh, J.K. Yoon and I.Y. Ko, Scripta Materialia. 58 (2008) 425-461.
26. C. Suryanarayana and M. Grant Norton, X-ray Diffraction A Practical Approach, Plenum Press, New York, 1998.
27. G.R. Anstis, P. Chantikul, B.R. Lawn and D.B. Marshall, J. Am. Ceram. Soc. 64 (1981) 533-541.
28. K. Robert, Wade, J. Am. Ceram. Soc. 75 (1992) 1682-1687.